Essential mechanisms in the triton binding

R. A. Brandenburg,[a],[b],[c] G. S. Chulick,[a],[d] R. Machleidt,[a],[e] A. Picklesimer,[a] and R. M. Thaler[a],[d]
[a]*Physics Division, Los Alamos National Laboratory, Los Alamos, New Mexico 87545*
[b]*Department of Physics, University of Basel, Basel, Switzerland*
[c]*Department of Physics, Purdue University, West Lafayette, Indiana 47907*
[d]*Physics Department, Case Western Reserve University, Cleveland, Ohio 44106*
[e]*Department of Physics, University of California at Los Angeles, Los Angeles, California 90024*
(Received 31 August 1987)

The recent successful prediction of the triton binding energy, E_t, with the static Bonn potential is examined. Modified versions of the potential are introduced to isolate separately the effects of the deuteron D-state admixture and the $^1S_0$ scattering length on E_t. Within this model study we find a monotonic relation between E_t and the $^1S_0$ scattering length and a strict linear dependence of E_t on the D-state admixture, in accordance with general well-known trends and earlier separable-potential model studies. The mechanism through which the weaker tensor force (lower D-state admixture) leads to a stronger binding of the triton is investigated by the introduction and study of effective energy-dependent central potentials.

Recently, successful microscopic predictions of the triton binding energy (E_t) based only upon realistic two-body forces have been reported.[1-3] These predictions, obtained with energy-independent parametrizations of the full meson-theoretic Bonn interaction,[4] are important because they mark a departure from previous indications that microscopic two-body forces are fundamentally inadequate to describe the triton binding.[5] The difference between these recent predictions and previous ones reflects an uncertainty in our ability to predict E_t due to ambiguities in the character of the two-body nucleon-nucleon (NN) input. A key issue, then, is the degree to which crucial features of the NN input are constrained by data and the extent to which unconstrained model dependencies internal to the two-body system can affect predictions of the triton binding energy. In order to address this issue, a precise characterization of the essential mechanisms which govern the triton binding is required. We need to know what aspect of the interaction is responsible for variations in predictions, and whether or not this feature of the NN interaction is a direct consequence of the NN data and of the basic assumptions of the theoretical model. In this paper we report the results of several numerical studies which we have performed to address these questions.

As a preliminary, we show in Table I the results of calculations of the triton binding energy with some of the "standard" realistic NN interactions,[6-10] along with our own recent results.[1] The "realistic" two-body interactions presented in Table I all provide accurate representations of the NN data.[11-15] Without this common prerequisite, it would, of course, be meaningless to compare their trinucleon predictions. Nevertheless, there are differences among these models, even on-shell. We summarize the bound-state and some low-energy scattering observables in Table I along with the deuteron S-D admixture, the so-called deuteron percent D state (P_D), predicted by the various models. Although the asymptotic deuteron D/S ratio η and the deuteron quadrupole moment are experimental observables which do constrain P_D, the percent D state is not directly observable and varies for reasonable models of the NN interaction from perhaps 4 to 7%.[4] That this is a principal ambiguity in the description of the NN interaction, which also has a strong effect in the trinucleon system, has long been known.[5] In fact it is this P_D ambiguity, which is closely related to ambiguities in the characterization of the NN tensor force, that is commonly accepted as the most important NN source of uncertainty in triton binding predictions. The main purpose of what follows is to clarify and further quantify the close relationship between the predicted values of P_D and E_t as well as the mechanisms responsible for this relationship.

The static momentum-space Bonn interaction of Ref. 4 (OBEPQ) forms the basis for the studies in this paper. As may be seen from Table I, this potential provides an excellent description of the important low-energy NN observables. It also yields a good description of low-energy phase-shift data as well as a faithful (on-shell) representation of the full Bonn interaction up to about 150 MeV (see Ref. 4, Sec. 9.3). Beyond about 150 MeV both of the static Bonn interactions, OBEPQ and its local r-space counterpart OBEPR, deviate appreciably from the full interaction in predictions for some partial waves, particularly for the ϵ_1 mixing parameter. The 325-MeV ϵ_1 prediction of the full Bonn interaction itself lies considerably below the commonly accepted value, although it may be argued that the empirical value of ϵ_1 is uncertain at least to this extent.[16] The static Bonn interactions substantially underpredict the full interaction above 150 MeV [e.g., ϵ_1 (325 MeV)=0.47° and −0.84°, for OBEPQ and OBEPR, respectively]. However, it is not yet known what significance to attach to these high-energy deviations in relation to low-energy trinucleon applications.

TABLE I. Two- and three-body system parameters calculated from the static momentum-space Bonn potential and from various static configuration-space potentials. Experimental deuteron and NN scattering parameters are from Refs. 12–15.

Quantity	Experiment	Bonn (Ref. 4)	Paris (Ref. 7)	SSC (Ref. 8)	RSC (Ref. 6)	$V14$ (Ref. 9)	TRS (Ref. 10)
Triton							
E_t (MeV)	8.48	8.35	7.64	7.53	7.35	7.67	7.56
Deuteron							
E_d (MeV)	−2.224 575(9)	−2.224 58	−2.2249	−2.224	−2.2246	−2.2250	−2.2245
P_D		4.38	5.77	5.45	6.47	6.08	5.92
Q_d (fm^2)	0.2859(3)	0.274[a]	0.279[a]	0.279[a]	0.2796[a]	0.286[a]	0.282[a]
μ_d (μ_N)	0.857 406(1)	0.8548[a]	0.853[a]	0.858[a]		0.845[a]	0.854[a]
A_S	0.8846(16)	0.8862	0.8869	0.8969	0.8776	0.8911	0.8884
A_S/A_D	0.0256(4)	0.0262	0.0261	0.0255	0.0262	0.0266	0.0262
r_d (fm)	1.9560(68)	1.9684	1.9716	1.9915	1.9567	1.98	1.9754
$^3S_1$ np scattering parameters							
a_t (fm)	5.424(4)	5.424	5.427	5.482	5.39	5.45	5.453
r_t (fm)	1.759(5)	1.760	1.766	1.833	1.720	1.80	1.797
$^1S_0$ NN scattering parameters							
a_{np} (fm)	−23.75(1)	−23.74				−23.67	
r_{np} (fm)	2.75(5)	2.70				2.77	
a_{pp}^c (fm)	−17.1(2)[b]		−17.61		−17.1		
r_{pp}^c (fm)	2.84(3)[b]		2.88		2.80		
a_{pp} (fm)	−7.828(8)		−7.810	−7.818	−7.78		−7.823
r_{pp} (fm)	2.80(2)		2.797	2.713	2.72		2.729

[a] Does not include meson exchange current contribution.
[b] Includes corrections for electromagnetic effects.

For example, it appears that an accurate representation of both the full interaction and the experimental data at low energies is more relevant for trinucleon bound-state properties. This is supported by the fact that OBEPQ and OBEPR predict[1,2] nearly identical triton binding energies despite the differences in their predictions for high-energy NN scattering parameters. Thus, both because of its intimate relationship with the full Bonn interaction and because of its excellent description of the energy regime below about 150 MeV, we regard OBEPQ as a "realistic" potential for our purposes.

The results of trinucleon calculations are conventionally classified according to the channels which are incorporated in the calculations. A channel corresponds to the coupling of a specific angular momentum state (LSJ) of an interacting pair of nucleons to a specific angular momentum state (lsj) of the spectator nucleon to produce, e.g., the triton $\mathcal{J}=\frac{1}{2}$. The choice of which channels to include and which to omit is somewhat arbitrary, but certain choices have become standard. Typically one specifies a maximum value of J and decides whether or not to include odd-parity NN states. For example, given ($J\leq 1$; $\pi=+$), ($J\leq 2$; $\pi=+$), ($J\leq 2$; $\pi=\pm$), or ($J\leq 4$; $\pi=\pm$), one has 5, 9, 18, or 34 channels, respectively. Table II contains the channels which comprise the five-channel calculation. Of special interest here is the *two*-channel case, which includes only channels 1 and 2 of Table II. For the two-channel case under discussion only the two-body T matrices $t_{LL'}^{SJ}=t_{00}^{00}$ and $t_{LL'}^{SJ}=t_{00}^{11}$ contribute. Note that this is not equivalent to setting the NN tensor potential to zero, since the full triplet potential is used to generate the NN T matrices.

In Table III we show a channel decomposition of the triton binding energy predictions of the various two-body interactions. The bulk of the binding is already present in the two-channel calculation, and, moreover, most of the distinction between the predictions of the static Bonn interaction and those of the other realistic interactions is also already present in the two-channel Bonn calculation. Although higher partial waves contribute somewhat differently from one NN model to another, this is not the qualitatively important distinction. Since the only input to the two-channel triton calculation are the $^1S_0$ and $^3S_1$ two-body T matrices, the major differences between the

TABLE II. The three-body five-channel coupling scheme.

Channel number	Pair L	Pair S	Pair J	Spectator l	Spectator s	Spectator j
1	0	0	0	0	$\frac{1}{2}$	$\frac{1}{2}$
2	0	1	1	0	$\frac{1}{2}$	$\frac{1}{2}$
3	0	1	1	2	$\frac{1}{2}$	$\frac{3}{2}$
4	2	1	1	0	$\frac{1}{2}$	$\frac{1}{2}$
5	2	1	1	2	$\frac{1}{2}$	$\frac{3}{2}$

TABLE III. The triton binding energy in MeV calculated for 2 through 34 channels for the potentials discussed in Table I.

Potential	Number of channels 2	5	9	18	34
Bonn[a]	8.16	8.36	8.44	8.32	8.35
RSC[b]	6.59[a]	7.04[a]	7.21	7.23	7.35
Paris[c]		7.30		7.38	7.64
SSC[b]		7.46	7.52	7.49	7.53
$V14$[b]		7.44	7.57	7.57	7.67
TRS[b]		7.49	7.56	7.52	7.56

[a] This work and Ref. 1.
[b] Reference 27.
[c] References 2 and 28.

static Bonn model and the others evidently arise from differences in these S-wave T matrices.

It has long been known that the triton binding energy is sensitive to low-energy on-shell observables (particularly the $^3S_1$ and $^1S_0$ scattering lengths[17–21]) and P_D.[20–23] As displayed in Table I, there are small but significant two-body differences among the various realistic potential models, and these differences make it difficult to study the dependence of E_t on variations of an individual "observable" in a realistic potential model. To avoid this complication, we found it expedient to generate several variants[24] of the "static Bonn potential" which were as alike as possible, differing either in P_D or, alternatively, in the $^1S_0$ scattering length, but fitting all other low-energy parameters to high accuracy. This approach also ensures that the off-shell variations between different versions of the potential are minimal. The momentum-space static Bonn potential (OBEPQ) which forms the basis of this work is discussed at length in Ref. 4. The two- and five-channel predictions for the models with varying P_D (with $^1S_0$ scattering length, a_{np}) and the corresponding parameter variations which give rise to the "new" potential models are given in Tables IV and V, respectively.

The $^1S_0$ part of the interaction can be characterized by the $^1S_0$ scattering length it produces, and the $^3S_1$ part of the interaction by its P_D prediction. In Fig. 1 we show how the triton binding energy behaves as a function of the P_D for two values of the $^1S_0$ scattering length. Since this calculation, like its predecessors, ignores charge-dependent effects, there is an ambiguity as to what value should be used for the $^1S_0$ scattering length. The two straight lines in that figure correspond to $a_{pp}(^1S_0) = -17.1$ fm and $a_{np}(^1S_0) = -23.75$ fm. The difference in the binding of the triton, corresponding to this difference in the $^1S_0$ scattering length, is $E_t(a_{np}) - E_t(a_{pp}) = +0.37$ MeV. Further discussion of this point will appear elsewhere in a treatment of charge dependence.[25] The linear dependence of the triton binding energy with respect to P_D, when other variations are minimized, is displayed in Fig. 1. We emphasize that the only input to these two-channel calculations are the $^1S_0$ and $^3S_1$ parts of the NN T matrix.

TABLE IV. The two- and five-channel results for variations of the Bonn potential and for the Reid soft-core potential.

	P_D	E_t (MeV) Two-channel	Five-channel
Potential A[a]	4.38	8.16	8.36
Potential B[b]	5.03	7.87	8.14
Potential C[b]	5.60	7.62	7.94
RSC	6.47	6.59	7.04

[a] OBEPQ of Ref. 4; see Table V for parameters.
[b] See Table V for parameters.

In view of the fact that the bulk of the triton binding is already given by the two-channel calculation, we expect the same linear dependence on P_D in the five-channel case. The cognate results for the five-channel calculation are plotted in Fig. 2. On this same figure we also show the points corresponding to the other models. The scatter represents a measure of the cumulative effect of the other differences beyond P_D in those models.

The foregoing also demonstrates that, apart from variations induced by differing $^1S_0$ scattering-length fits, we can focus on the $^3S_1$ NN partial wave as the principal source of the distinction between the new results and earlier ones. That the bulk of the difference between models is already present at the two-channel level implies that the tensor part of the T matrix does not play a crucial role. The essential conduit is the diagonal $^3S_1$ T matrix, and the principal effects of different tensor-central potential admixtures of the various models evidently resides therein. To clarify the mechanism through which this proceeds, we observe that the central and tensor forces are both attractive in the even parity $J=1$ state, and that different realistic forces achieve the same ~ 2.2 MeV binding energy of the deuteron through different relative strengths of their central and tensor parts. A stronger central force necessarily implies a weaker tensor force, and vice versa, in order to achieve the observed deuteron binding energy. This is illustrated in Fig. 3, where the central and tensor parts of two different local potentials, which fit the deuteron and low-energy triplet scattering observables, are plotted. Such a local potential is discussed in Ref. 4. Although the properties of local potentials are the most easily depicted, the properties we are discussing are shared by a much wider class of static interactions. From Fig. 3 it is evident that the model with the stronger central force has the weaker tensor force (lower P_D).

In the triton the tensor force apparently contributes relatively less to the binding than does the central force in order to produce the observed correlation: that a lower P_D leads to a more strongly bound triton. We want to examine more closely the mechanism by which, all other things being equal, a stronger tensor force implies a weaker triton binding.

The NN $^3S_1$ T matrix, $T^S(E)$, enters into the Faddeev triton binding calculation for values of the parametric energy $E = -E_t - \frac{3}{4}q^2/m$, where E_t (~ 8.0 MeV) is the triton binding energy, m is the nucleon mass, and q is the magnitude of the momentum of the spectator nucleon relative to the interacting pair. In general the Faddeev cal-

TABLE V. Parameters used to construct the three variants of the static momentum-space Bonn potential used in this paper. Potential *A* is OBEPQ of Ref. 4; potentials *B* and *C* are from Ref. 24.

Meson	$I^G(J^{PC})$	m_α (MeV)	Potential	Potential dependent parameters $g_\alpha^2/4\pi$; (f_α/g_α)	Λ_α (GeV)	$(n_\alpha)^a$
			$T=1$ parameters			
π	1^- (0^{-+})	138.03	*A*	14.6	1.3	1.0
			B	14.4	1.7	1.0
			C	14.2	3.0	1.0
η	0^+ (0^{-+})	548.8	*A*	5.0	1.5	1.0
			B	5.0	1.5	1.0
			C	0.0	1.5	1.0
ρ	1^+ (1^{--})	769.0	*A*	0.81; (6.1)	2.0	2.0
			B	0.90; (6.1)	1.63	1.5
			C	1.00; (6.1)	1.7	2.0
ω	0^- (1^{--})	782.6	*A*	20.0; (0.0)	1.5	1.0
			B	20.0; (0.0)	1.5	1.0
			C	22.0; (0.0)	1.5	1.0
δ	1^- (0^{++})	983.0	*A*	1.1075	2.0	1.0
			B	2.2246	2.0	1.0
			C	4.6090	2.0	1.0
σ	0^+ (0^{++})	550.0	*A*	8.2797	2.0	1.0
			B	8.0117	2.0	1.0
			C	8.4806	1.8	1.0
			$T=0$ parameters			
			same as for $T=1$, except for			
σ	$0^+(0^{++})$	720.0	*A*	16.9822	2.0	1.0
		740.0	*B*	18.3251	2.0	1.0
		720.0	*C*	17.6140	2.0	1.0

[a] Power of vertex form factor $F_\alpha[(\mathbf{k})^2]=[(\Lambda_\alpha^2-m_\alpha^2)/(\Lambda_\alpha^2+\mathbf{k}^2)]^{n_\alpha}$.

culation samples the T matrix far off-shell and at very negative energies with the most important range being perhaps -60 MeV $< E < -10$ MeV, in consonance with typical nuclear bound-state behavior. Note that we leave the energy range in which data constrain the various potential models as soon as E decreases below the deuteron binding. Below this point, the contributions to $T^S(E)$ from a tensor force may be expected to be weakened.

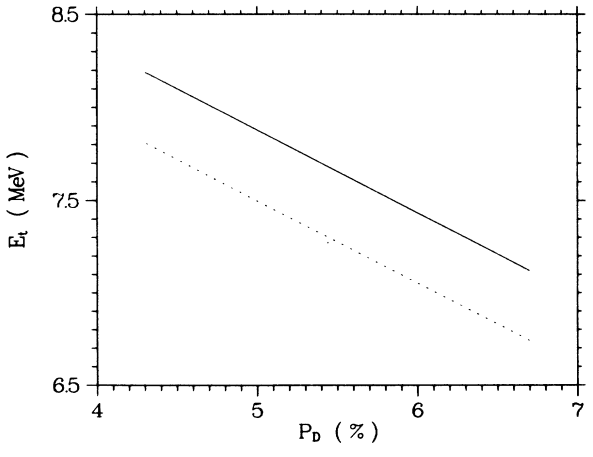

FIG. 1. The two-channel E_t as a function of P_D. The solid line corresponds to a_{np} and the dotted line corresponds to a_{pp}.

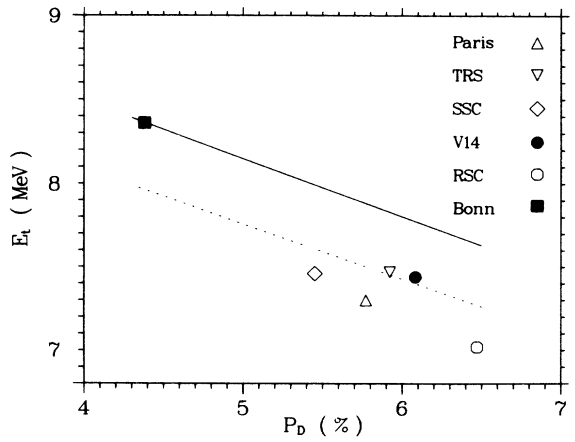

FIG. 2. Same as Fig. 1 for the five-channel calculations.

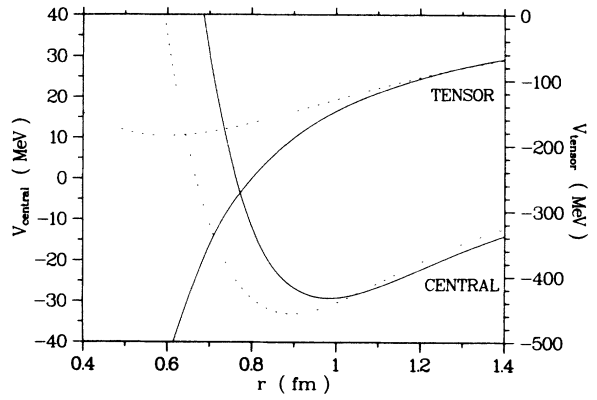

FIG. 3. The central and $^3S_1$-$^3D_1$ tensor forces for two local coordinate-space potentials, one with $P_D=5.3\%$ (solid line) and the other with $P_D=4.8\%$ (dotted line).

The reason for this is that the T matrix satisfies the Lippmann-Schwinger equation

$$T(E)=V+VG_0(E)T(E)\ , \tag{1}$$

where V denotes the underlying potential, the Green's function G_0 is $(E-h_0+i\epsilon)^{-1}$, and h_0 denotes the kinetic energy operator. Thus, if we project out the diagonal $^3S_1$ T matrix, $T^S=\langle {}^3S\mid T(E)\mid {}^3S\rangle$ or simply $\langle S\mid T(E)\mid S\rangle$, we find

$$T^S(E)=V^S+V^SG_0(E)T^S(E)+V^{SD}G_0(E)T^{DS}(E)\ , \tag{2}$$

where V^S is the diagonal ^3S potential (which is purely central since the tensor force cannot contribute), V^{SD} is the S to D transition potential (necessarily the tensor potential V_T), so that Eq. (2) can be expressed as

$$T^S(E)=V_c^S+V_c^SG_0(E)T^S(E)+V_T^{SD}G_0(E)T^{DS}(E)\ . \tag{3a}$$

The associated transition T-matrix element $T^{DS}(E)$ satisfies

$$T^{DS}(E)=V_T^{DS}+V_T^{DS}G_0(E)T^S(E)+V^DG_0(E)T^{DS}(E)\ , \tag{3b}$$

where V^D is just the diagonal D-wave interaction.

To see this qualitively, we expand Eq. (3a), and observe that the lowest-order central and tensor contributions to $T^S(E)$ are

$$T^S_{(1)}(E)=V_c^S+V_T^{SD}G_0(E)V_T^{DS}\ , \tag{4a}$$

or in momentum space,

$$T^S_{(1)}(k',k;E)=V_c^S(k',k)+\int V_T^{SD}(k',k'')G_0(k'',E)\times V_T^{DS}(k'',k)d^3k''\ , \tag{4b}$$

where

$$G_0(k'',E)=\left[E-\frac{k''^2}{2m}+i\epsilon\right]^{-1}\ . \tag{5}$$

Thus while there is a constant, energy-independent contribution to $T^S(E)$ from the central potential, its lowest-order tensor contribution contains an explicit energy dependence. Moreover, for the negative parametric energies of relevance to the triton binding, there is no pole in $G_0(E)$ and this tensor contribution progressively weakens as E increases. This candidate mechanism for explaining the correlation between weaker tensor forces and stronger triton binding energies is not new and has long been recognized, especially in the context of nuclear matter.[26]

To verify and further quantify this mechanism, we have made several numerical studies. The most obvious check is to look directly at the behavior of $T^S(E)$ as a function of E. One such case is shown in Fig. 4. Here we examine the behavior of $T^S(k,k;-k^2/2m)$ and observe the expected correlation between the strength of the tensor force and the weakening of T^S. However, the $^3S_1$ T matrix is a function of three independent variables and its behavior for different models and different surfaces (in the space of its independent variables) is rather complicated. Thus, although a sympathetic eye can discern the desired correlations in plots such as that of Fig. 4, this cannot really be considered conclusive. Another possibility is to examine the unique energy-dependent, effective central potential $U^S(E)=\langle S\mid U(E)\mid S\rangle$ which exactly reproduces $T^S(E)$ via

$$T^S(E)=U^S(E)+U^S(E)G_0(E)T^S(E) \tag{6}$$

or

$$U^S(E)=T^S(E)-T^S(E)G_0(E)U^S(E)\ . \tag{7}$$

The rationale for introducing $U^S(E)$ is simply that our intuition is better attuned to potentials than to T-matrix structure. Note from Eq. (3a) that if $V_T^{SD}=0$, then $U^S(E)$ is just V_c^S and is energy independent. In k space it is, in

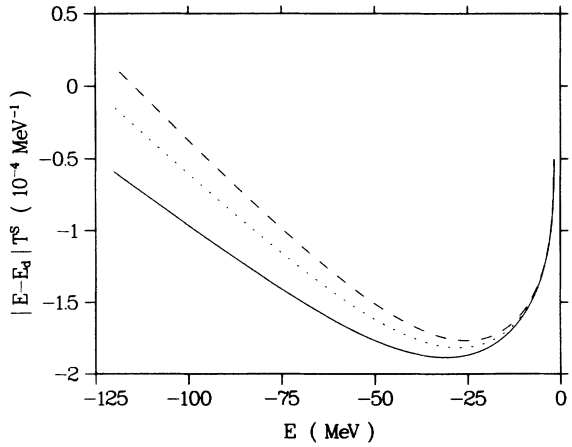

FIG. 4. The quantity $|E-E_d|\,T^S(k,k,E)$ plotted vs $E=-k^2/2m$. The factor $|E-E_d|$ is included to eliminate the deuteron pole. The solid line represents potential A, the dotted line represents potential B, and the dashed line represents potential C, all as given in Table V.

fact, a very simple matter to obtain this effective potential, $U^S(E)$, numerically. Given the solution $T^S(E)$ of Eq. (3a), one can solve Eq. (7) to find $U^S(E)$. One may then examine $U^S(k',k;E)$ in an effort to understand the observed correlation between tensor strength and triton binding. Unfortunately one again encounters the same difficulty as in the case of $T^S(k',k;E)$, namely, that $U^S(k',k;E)$ is a complicated function of three variables.

Let us nevertheless pursue the idea of an effective energy-dependent central potential somewhat further. If we use Eq. (3b) to eliminate $T^{DS}(E)$ from Eq. (3a) and then solve Eq. (3a), we find that $U^S(E)$ as defined by Eq. (6) is just

$$U^S(E)=V^S+V^{SD}G_0(E)\frac{1}{1-V^DG_0(E)}V_T^{DS}\ . \tag{8}$$

Notice that taking the Born approximation in Eq. (6) and neglecting the diagonal D-wave scattering [setting $V_D=0$ in Eq. (8)] we obtain the same approximation as in Eq. (4a). The advantage of $U^S(E)$ is that the implicit energy dependence associated with the tensor force has been made manifest and is thus available for direct manipulation. This allows us to obtain a direct measure of the weakening of the effective interaction between two nucleons as the parametric energy decreases, as follows. One may employ the effective central potential $U_S(E)$, with E treated simply as a parameter, to calculate the energy, $\beta(E)$ at which the two-nucleon system would bind for a variety of parameter choices E.

The quantity $\beta(E)$ can be understood as

$$\begin{aligned}\beta(E)&\equiv\langle\hat{\psi}\,|\,H^S(E)\,|\,\hat{\psi}\rangle/\langle\hat{\psi}/\hat{\psi}\rangle\\&=\langle\hat{\psi}\,|\,[h_0+U^S(E)]\,|\,\hat{\psi}\rangle/\langle\hat{\psi}\,|\,\hat{\psi}\rangle\ .\end{aligned}\tag{9}$$

With the physical deuteron energy E_d as a reference point,

$$\begin{aligned}\beta(E)&=\{\langle\hat{\psi}\,|\,[h_0+U^S(E_d)]\,|\,\hat{\psi}\rangle\\&\quad+\langle\hat{\psi}\,|\,[U^S(E)-U^S(E_d)]\,|\,\hat{\psi}\rangle\}/\langle\hat{\psi}\,|\,\hat{\psi}\rangle\\&=\langle\{\hat{\psi}\,|\,H^S(E_d)\,|\,\hat{\psi}\rangle\\&\quad+\langle\hat{\psi}\,|\,[U^S(E)-U^S(E_d)]\,|\,\hat{\psi}\rangle\}/\langle\hat{\psi}\,|\,\hat{\psi}\rangle\ .\end{aligned}\tag{10}$$

In Eqs. (9) and (10) above h_0 is the kinetic-energy operator and $|\,\hat{\psi}\rangle$ is defined through the eigenvalue equation $H^S(E)\,|\,\hat{\psi}(E)\rangle=\beta(E)\,|\,\hat{\psi}(E)\rangle$. If $|\,\hat{\psi}\rangle$ in Eqs. (9) and (10) may be considered to be normalized and may be reasonably closely approximated by $|\,\psi(E_d)\rangle$, then we may approximate Eq. (10) as

$$\beta(E)\approx\beta(E_d)+\langle\hat{\psi}\,|\,[U^S(E)-U^S(E_d)]\,|\,\hat{\psi}\rangle \tag{11}$$

so that

$$\begin{aligned}\beta(E)-\beta(E_d)&\cong\langle\psi(E_d)\,|\,[U^S(E)-U^S(E_d)]\,|\,\psi(E_d)\rangle\\&=\langle\psi(E_d)\,|\,\Delta U^S(E)\,|\,\psi(E_d)\rangle\ .\end{aligned}\tag{12}$$

Thus $\beta(E)$ is a direct measure of the strength of the effective potential approximately weighted by the deuteron momentum distribution, and $\beta(E)-\beta(E_d)$ is a measure of the weakening of the effective central force as the parametric energy decreases below E_d. The results of this study are plotted in Fig. 5 for our typical examples of variable tensor forces. All of the curves converge to the correct value of β when $E=E_d$, as they must to yield the physical deuteron binding in the various models [i.e., $U^S(E_d)$ necessarily correctly yields E_d].

We have also made similar studies in which we have used the low-order, energy-dependent T matrix $T^S_{(1)}(E)$ in place of $T^S(E)$. If, however, $T^S_{(1)}(E)$ is substituted for $T^S(E)$ in Eq. (7) to give $U^S_1(E)$, we find that the predicted values of $\beta(E)$ for $E=E_d$ (the deuteron bound-state energy) for the various models already deviated from E_d by as much as 0.5 MeV. Thus, although the first-order argument as to the contribution of the tensor force to the energy dependence of $T^S(E)$ is qualitatively correct, the neglected higher-order terms $[T^S(E)-T^S_1(E)]$ are essential to the observed effect.

The striking features of Fig. 5 are twofold. First, for each of the models for energies below E_d, the effective strength of the interaction decreases monotonically with E. Thus $T^S(E)$ represents a T matrix which corresponds to an ever-weakening potential $U^S(E)$ as the parametric energy E decreases over its range of allowed values in the triton calculation. This implies, of course, that as the momentum of the spectator nucleon relative to the interacting pair increases, the contribution to the triton binding becomes weakened. The decrease in average potential strength as E moves from E_d to about -100 MeV is about 1.5 to 2.0 MeV for the range of models (4–7 % D state) under consideration. Second, as the P_D associated with the various static potentials increases, the effective strength of the interaction decreases monotonically, for all $E<E_d$, i.e., the curves in Fig. 5 do not cross.

Thus, in the calculation of the triton binding energy, as $T^S(E)$ is sampled over its parametric dependence on E, the stronger the tensor force of the model, the weaker the effective potential associated with $T^S(E)$ *for all* E relevant to the triton calculation. Hence, one is justified in making the simple statements: (1) the energy-

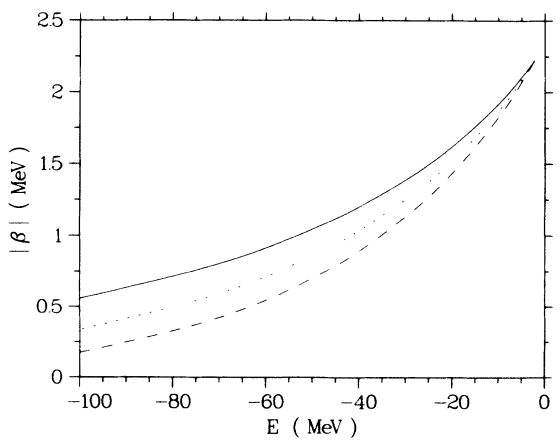

FIG. 5. The binding energy of the "deuteron" as calculated with the effective potential $U^S(E)$ plotted versus the energy parameter E. The curves are coded as in Fig. 4.

dependent effective potentials associated with stronger tensor forces are weaker and (2) triton $^3S_1$ channels everywhere "see" weaker forces for stronger tensor potentials.

These conclusions are further illustrated by the two-channel calculation of the triton binding energy displayed in Fig. 6. There we have used the effective potential $U^S(E)$ at a fixed value of the parametric energy E, along with the energy-independent singlet S potential, to obtain the triton binding energy. We show three curves characterized by different values of P_D. Along the abscissa are the values of the parameter E in the effective interaction $U^S(E)$, now treated as a static interaction; the ordinates are the calculated triton binding energies. Figure 6 is the three-body analog to Fig. 5. The particular "average" values of E that yield the identical values of E_t to those in Table IV are marked. For these cases we see that this average energy is just above -20 MeV and increases with increasing P_D. The similarity of the curves in Fig. 6 to those in Fig. 5 illustrates the close connection between the role of the tensor force in $\beta(E)$ and in the binding energy of the triton.

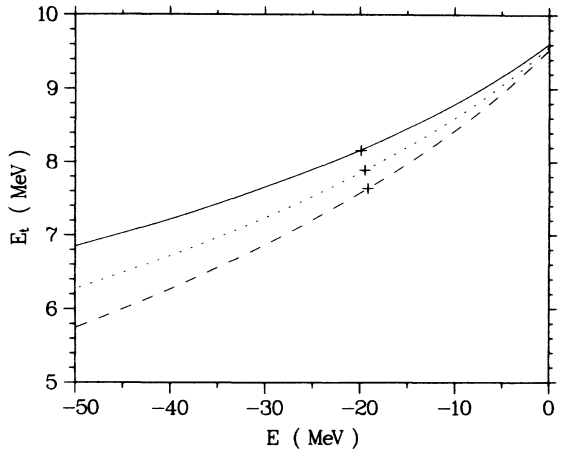

FIG. 6. The two-channel E_t for different effective interactions $U^S(E)$, used as static potentials, plotted versus the parametric energy E. The curves are coded as in Fig. 4.

In summary, we have recently shown that the energy-independent approximation to the full Bonn interaction successfully predicts the triton binding energy. In order to dissect the reasons for this departure from previous failures by two-body forces, we have manufactured several variants of the static Bonn interaction whose primary differences lie in differing tensor strengths, as reflected by differing predictions of P_D (the deuteron percent D state). It turns out that the main distinction between the static Bonn interaction and other realistic interactions is already reflected in the results for a two-channel (S-wave pair interaction) Faddeev calculation. Variations in the $^1S_0$ contribution to the triton binding were characterized and reveal that it is the difference in the $^3S_1$ contribution which provides the essential new aspect. We find a linear relationship between E_t and P_D, a more precise version of a well-known correlation. We then investigate the way in which the $^3S_1$ T matrix $[T^S(E)]$ element carries this information in a triton calculation. By defining an energy-dependent, effective central potential $U^S(E)$, we replace the effect of the tensor character of the underlying potential by an explicit energy dependence. This allows us to gauge the strength of the potential which the triton calculation sees over the allowed range of parametric energies $E < -E_t$. Figure 5 then illustrates graphically that (1) as E decreases the attraction decreases monotonically and (2) that stronger tensor forces monotonically imply weaker effective attraction for all $E < -E_t$. Comparison of Figs. 5 and 6 shows that the value of E_t for a given model scales with the strength of $U^S(E)$ at each E, though not uniformly, and that E_t and the strength of $U^S(E)$ show essentially identical dependences upon P_D, demonstrating that $U^S(E)$ serves as a conduit for the tensor-induced variations in E_t, a result expected on the basis of perturbative considerations. This provides a clear picture of the mechanism by which variations in the tensor/central strength of potential models modify predicted values of the triton binding energy, in general, and make manifest the source of the success of the recent triton predictions as the influence of the low P_D of the static Bonn potential (4.38%) on the $^3S_1$ T matrix.

This work was supported in part by the U.S. Department of Energy. One of us (R.A.B.) was supported by the U.S. National Science Foundation. The Los Alamos National Laboratory is operated by the University of California for the U.S. Department of Energy under Contract No. W-7405-ENG-36.

[1]R. A. Brandenburg, G. S. Chulick, R. Machleidt, A. Picklesimer, and R. M. Thaler, Los Alamos National Laboratory Report No. LA-UR-86-3700, 1986 (unpublished).
[2]T. Sasakawa, Nucl. Phys. **A463**, 327c (1987).
[3]R. Machleidt, Bull. Am. Phys. Soc. **32**, 1114 (1987); G. S. Chulick, R. A. Brandenburg, R. Machleidt, A. Picklesimer, and R. M. Thaler, *ibid.* **32**, 1058 (1987).
[4]R. Machleidt, K. Holinde, and C. Elster, Phys. Rep. **149**, 1 (1987).
[5]See, for example, J. L. Friar, B. F. Gibson, and G. L. Payne, Comments Nucl. Part. Phys. **11**, 51 (1983); G. L. Payne, J. L. Friar, and B. F. Gibson, Phys. Rev. Lett. **55**, 374 (1985); C. R. Chen, G. L. Payne, J. L. Friar, and B. F. Gibson, Phys. Rev. C **33**, 401 (1986).
[6]R. V. Reid, Ann. Phys. (N.Y.) **50**, 411 (1968).
[7]M. Lacombe *et al.*, Phys. Rev. C **21**, 861 (1980).
[8]R. de Tourreil and D. W. L. Sprung, Nucl. Phys. **A201**, 193 (1973).
[9]R. B. Wiringa, R. A. Smith, and T. A. Ainsworth, Phys. Rev. C **29**, 1207 (1984).

[10]R. de Tourreil, B. Rouben, and D. W. L. Sprung, Nucl. Phys. **A242**, 445 (1975).
[11]W. T. H. van Oers, Nucl. Phys. **A463**, 517c (1987).
[12]T. E. O. Ericson and M. Rosa-Clot, Nucl. Phys. **A405**, 497 (1983).
[13]S. Klarsfeld, J. Martorell, and D. W. L. Sprung, J. Phys. G **10**, 165 (1984).
[14]N. L. Rodning and D. L. Knutson, Phys. Rev. Lett. **57**, 2248 (1986).
[15]O. Dumbrajs *et al.*, Nucl. Phys. **B216**, 277 (1983).
[16]G. S. Chulick, C. Elster, R. Machleidt, A. Picklesimer, and R. M. Thaler, Phys. Rev. C (to be published).
[17]V. F. Kharchenko, N. M. Petrow, and S. A. Storozhenko, Nucl. Phys. **A106**, 464 (1968).
[18]B. F. Gibson and G. J. Stephenson, Jr., Phys. Rev. C **8**, 122 (1973).
[19]M. Orlowski and Y. E. Kim, Phys. Rev. C **32**, 1376 (1985).
[20]I. R. Afnan and J. M. Read, Phys. Rev. C **12**, 293 (1975).
[21]A. C. Philips, Rep. Prog. Phys. **40**, 905 (1977).
[22]A. C. Philips, Nucl. Phys. **A107**, 209 (1968).
[23]M. Orlowski, Phys. Rev. C **32**, 660 (1985).
[24]R. Machleidt, Adv. Nucl. Phys. (to be published).
[25]R. A. Brandenburg, G. S. Chulick, Y. E. Kim, D. J. Klepaki, R. Machleidt, A. Picklesimer, and R. M. Thaler, Phys. Rev. C **37**, 781 (1988).
[26]M. I. Haftel and F. Tabakin, Nucl. Phys. **A158**, 1 (1970).
[27]C. R. Chen, G. L. Payne, J. L. Friar, and B. F. Gibson, Phys. Rev. C **31**, 2266 (1985).
[28]C. Hajduk and P. U. Sauer, Nucl. Phys. **A369**, 321 (1981).